

## Supplementary Information

### Structural perspective on revealing heat dissipation behavior of CoFe<sub>2</sub>O<sub>4</sub>-Pd nanohybrids: A great promise for magnetic fluid hyperthermia

**S. Fatemeh Shams,<sup>1,\*</sup> Mohammad Reza Ghazanfari,<sup>2</sup> Susanne Pettinger,<sup>3,4,5</sup> Amir H. Tavabi,<sup>6</sup> Konrad Siemensmeyer,<sup>7</sup> Alevtina Smekhova,<sup>1,#</sup> Rafal E. Dunin-Borkowski,<sup>6</sup> Gil G. Westmeyer,<sup>3,4,5</sup> Carolin Schmitz-Antoniak<sup>1</sup>**

1. Peter-Grünberg-Institut (PGI-6), Forschungszentrum Jülich, 52425 Jülich, Germany

2. Institute of Chemistry and Biochemistry, Freie Universität Berlin, 14195 Berlin, Germany

3. Institute of Biological and Medical Imaging, Helmholtz Zentrum München, 85764 Neuherberg, Germany

4. Institute of Developmental Genetics, Helmholtz Zentrum München, 85764 Neuherberg, Germany

5. Department of Nuclear Medicine, TUM School of Medicine, Technical University of Munich, 81675 Munich, Germany

6. Ernst Ruska-Centre for Microscopy and Spectroscopy with Electrons and Peter Grünberg Institut, Forschungszentrum Jülich, 52425 Jülich, Germany

7. Helmholtz-Zentrum Berlin für Materialien und Energie, 14109 Berlin, Germany

# Present address: Helmholtz-Zentrum Berlin für Materialien und Energie, 12489 Berlin, Germany

\*Corresponding author:

Dr. S. Fatemeh Shams

E-mail: f.shams@fz-juelich.de

Phone: +49 30 8062 14779

#### S1. Characteristics of samples used to measure SAR values of bare CFO and CFO-Pd nanoparticles

In this section, the structural and microstructural features of nanoparticles studied to evaluate particle-size-dependent fluid heating and to optimize synthesis process are presented. The SAR values is also plotted as a function of particle size curve. CFO nanoparticles were synthesized with twenty different ranges of hydrodynamic diameter between 7.20 and 40 nm. The measured hydrodynamic size, size distribution, polydispersity index (PDI) and crystallite size determined using DLS and XRD are listed in Table S1. Tables S2 and S3 list the CFO and CFO-Pd samples and measurements parameter used to study concentration / field amplitude-dependent fluid heating.

Table S1. Characteristics of samples used for size-dependent SAR measurements: mean hydrodynamic diameter  $d_H$ , hydrodynamic size distribution  $D_V$ , hydrodynamic polydispersity index PDI and crystallite diameter  $d_{Cryst}$ .

| Composition | $d_H$ (nm) | $D_V$ (nm) | PDI   | $d_{Cryst}$ (nm) |
|-------------|------------|------------|-------|------------------|
| CFO         | 7.20       | 2.70       | 0.071 | 5.80             |
| CFO         | 10.24      | 3.10       | 0.078 | 8.25             |
| CFO         | 11.04      | 3.40       | 0.075 | 8.89             |
| CFO         | 11.50      | 3.50       | 0.080 | 9.26             |
| CFO         | 11.61      | 3.90       | 0.081 | 9.35             |
| CFO         | 12.05      | 4.20       | 0.079 | 9.71             |
| CFO         | 12.17      | 4.20       | 0.078 | 9.80             |
| CFO         | 12.80      | 4.70       | 0.084 | 10.31            |
| CFO         | 13.70      | 4.90       | 0.085 | 11.04            |
| CFO         | 14.18      | 5.00       | 0.082 | 11.42            |
| CFO         | 14.40      | 5.20       | 0.086 | 11.62            |
| CFO         | 14.77      | 5.30       | 0.088 | 11.90            |
| CFO         | 15.56      | 5.80       | 0.093 | 12.57            |
| CFO         | 15.70      | 6.10       | 0.091 | 12.65            |
| CFO         | 15.92      | 6.10       | 0.089 | 12.82            |
| CFO         | 17.51      | 7.10       | 0.082 | 14.11            |
| CFO         | 17.77      | 7.30       | 0.090 | 14.39            |
| CFO         | 24.10      | 7.80       | 0.084 | 19.41            |
| CFO         | 31.00      | 8.10       | 0.078 | 24.97            |
| CFO         | 40.00      | 8.50       | 0.086 | 32.22            |

Table S2. Values of fluid concentration, magnetic field amplitude and magnetic field frequency used in the present studies of CFO nanoparticles of different diameter.

| Composition | $d_H$ (nm) | Concentration (mg/ml) | Magnetic field amplitude (mT) | Magnetic field frequency (kHz) |
|-------------|------------|-----------------------|-------------------------------|--------------------------------|
| CFO         | 7.20       | 1                     | 12                            | 318                            |
|             |            | 15                    | 19                            |                                |
| CFO         | 10.24      | 1                     | 12                            | 318                            |
|             |            | 15                    | 19                            |                                |
| CFO         | 11.04      | 15                    | 19                            | 318                            |
| CFO         | 12.17      | 15                    | 19                            | 318                            |
| CFO         | 13.70      | 1                     | 12                            | 318                            |
|             |            | 15                    | 19                            |                                |
| CFO         | 14.77      | 15                    | 19                            | 318                            |
| CFO         | 15.70      | 15                    | 19                            | 318                            |
| CFO         | 17.77      | 1                     | 12                            | 318                            |
|             |            | 15                    | 19                            |                                |
| CFO         | 24.10      | 1                     | 12                            | 318                            |
|             |            | 15                    | 19                            |                                |

Table S3. Measurement parameters of the studied CFO and CFO-Pd nanoparticles.

| Composition | $d_H$ (nm) | Concentration (mg/ml) | Magnetic field amplitude (mT) | Magnetic field frequency (kHz) |
|-------------|------------|-----------------------|-------------------------------|--------------------------------|
| CFO         | 7.20       | 1                     | 19                            | 318                            |
| CFO         | 24.10      | 1                     | 19                            | 318                            |
| CFO-Pd      | 7.20       | 1                     | 19                            | 318                            |
| CFO-Pd      | 24.10      | 1                     | 19                            | 318                            |

All of the samples were qualitatively and quantitatively analyzed using XRD measurements to identify the chemical phases present and to investigate their structural characteristics. As an example, an XRD pattern and fitted Rietveld structure refinement for 7.20 nm nanoparticles are shown in Fig. S1. The Rietveld refinement was performed by applying the Reflex program to raw data from X-ray diffraction patterns for a 2-theta range between 20 ° and 80 °. The fitting process was carried out based on a reference file with CIF number 1533163. The  $R_{wp}$  value is below 10%, confirming the fitting and refinement process.

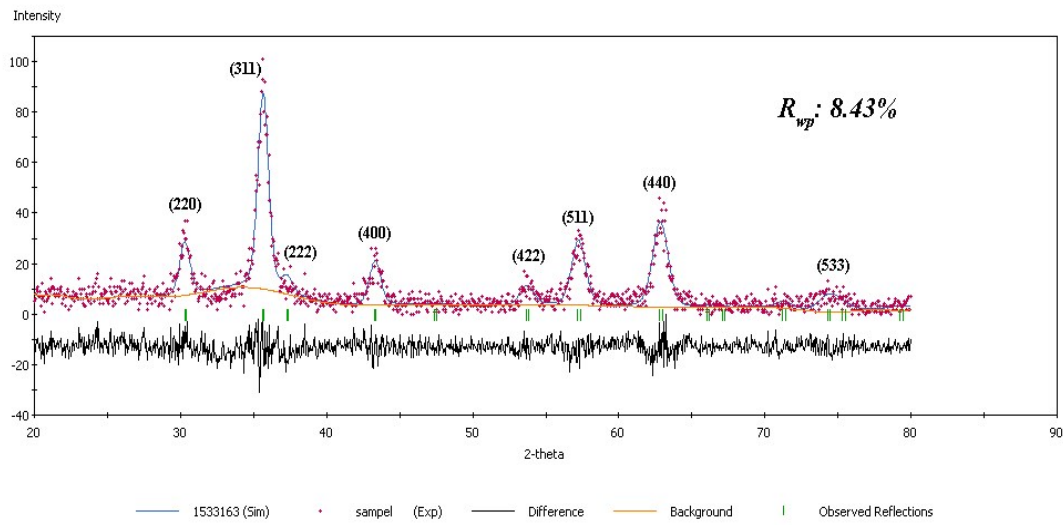


Figure S1. XRD pattern and fitted Rietveld structure refinement for 7.20 nm nanoparticles.

## S2. Magnetometry results

Figure S2 shows the mass magnetization as a function of DC magnetic field at  $T = 300$  K. The symbols show experimental data, while the lines show simulations for the high-field region (above 3 T) according to the well-established law of approach:

$$M = M_S \left( 1 - \frac{\alpha}{H^2} \frac{K_{eff}^2}{M_S^2} \right) + \chi_p H = M_S \left( 1 - \frac{\beta}{H^2} \right) + \chi_p H \quad (S1)$$

where  $M_S$  is the saturation magnetization and the susceptibility  $\chi_p$  accounts for additional linear contributions (the so-called paraprocess). For CFO nanoparticles, we assume that the effective magnetic anisotropy can be described as uniaxial in a first approximation and used the corresponding value  $\alpha = 4/15$ . (For cubic systems,  $\alpha = 8/105$ ). Following suggestions from Grössinger,<sup>S1</sup> the fitting

behavior was tested for various combinations of fitting parameters and in different field regions. Table S4 summarized the simulation parameters for the best fit to the experimental data and calculated values of the effective anisotropy constant per kg. In order to convert the values to SI units, as shown in Table 1 of the main manuscript, the mass magnetization, mass susceptibility and anisotropy constant per kg were multiplied by the density  $\rho = 5.3 \times 10^3 \text{ kg/m}^3$ .

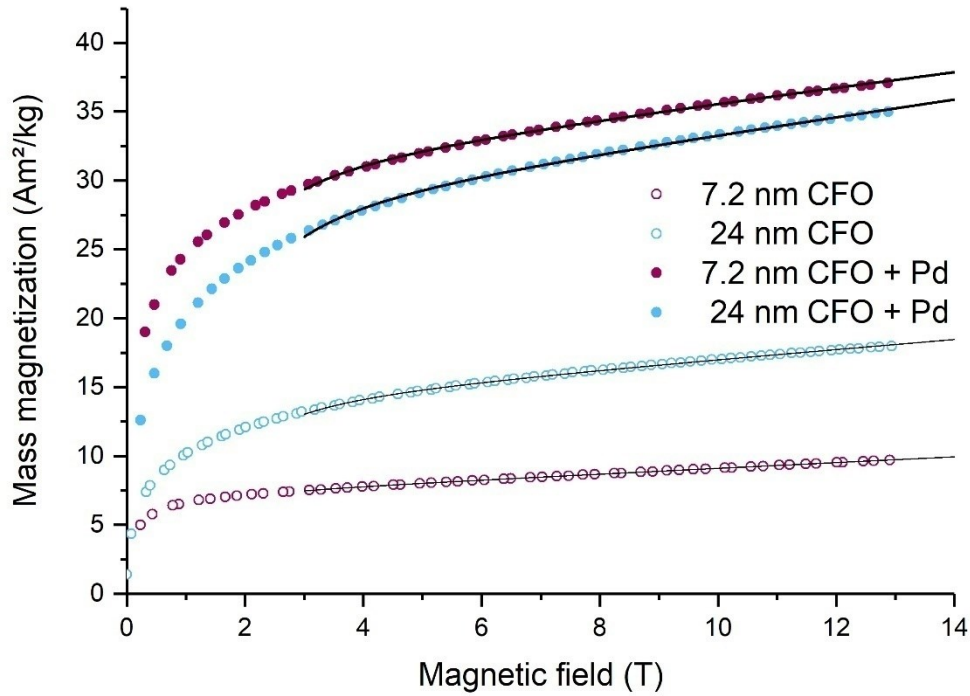


Figure S2. Mass magnetization plotted as a function of applied DC magnetic field at  $T = 300 \text{ K}$  for CFO nanoparticles with two different mean diameters and corresponding CFO-Pd heterodimers. The symbols correspond to experimental data, while the lines show simulations according to Eq. S1. For clarity, only every 150<sup>th</sup> point of the experimental data is plotted.

For both sizes of CFO nanoparticles, CFO-Pd heterodimers show enhanced saturation magnetization and enhanced magnetic anisotropy with respect to bare CFO nanoparticles. In addition, the factor  $\chi_p$  is larger for CFO-Pd heterodimers, which may indicate an additional contribution from paramagnetic Pd to the magnetometry data.

The magnetic mass susceptibility was calculated from the magnetometry data using the equation

$$\chi_m = \mu_0 \frac{\partial M_m}{\partial B}, \quad (S2)$$

where  $M_m$  is the mass magnetization (Fig. S2) and  $B$  is the applied magnetic field. Some spikes occur due to automatic position correction of the sample. The susceptibilities of the CFO-Pd heterodimers are again significantly larger than those of the bare CFO nanoparticles for both sizes, reaching values of up to  $3.0\text{-}3.5 \times 10^{-4} \text{ m}^3/\text{kg}$ .

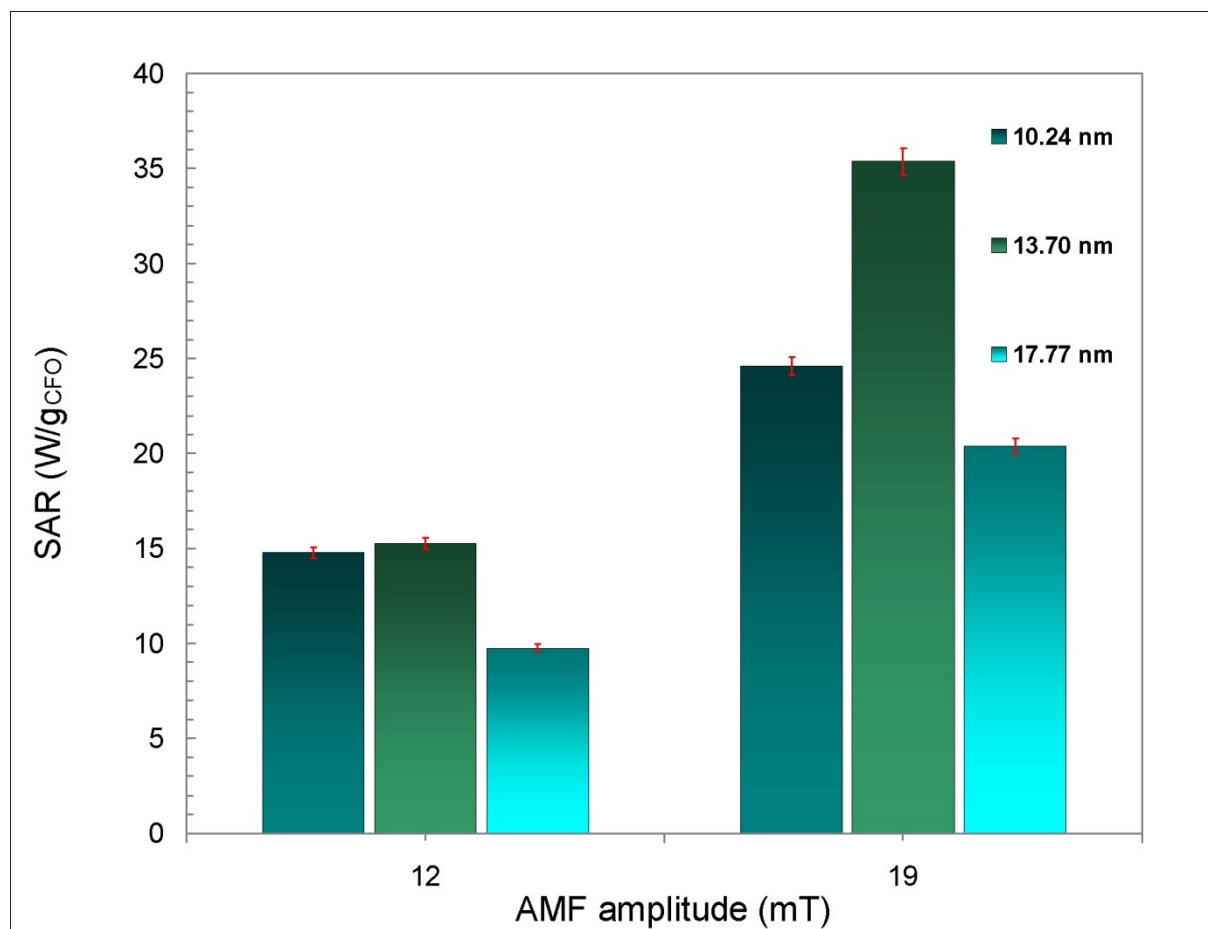


Figure S3. SAR values of CFO nanoparticle suspensions for three different particles sizes and two amplitudes of the AC magnetic field (12 and 19 mT). The fluids concentration and magnetic field frequency were 15 mg/ml and 318 kHz, respectively.

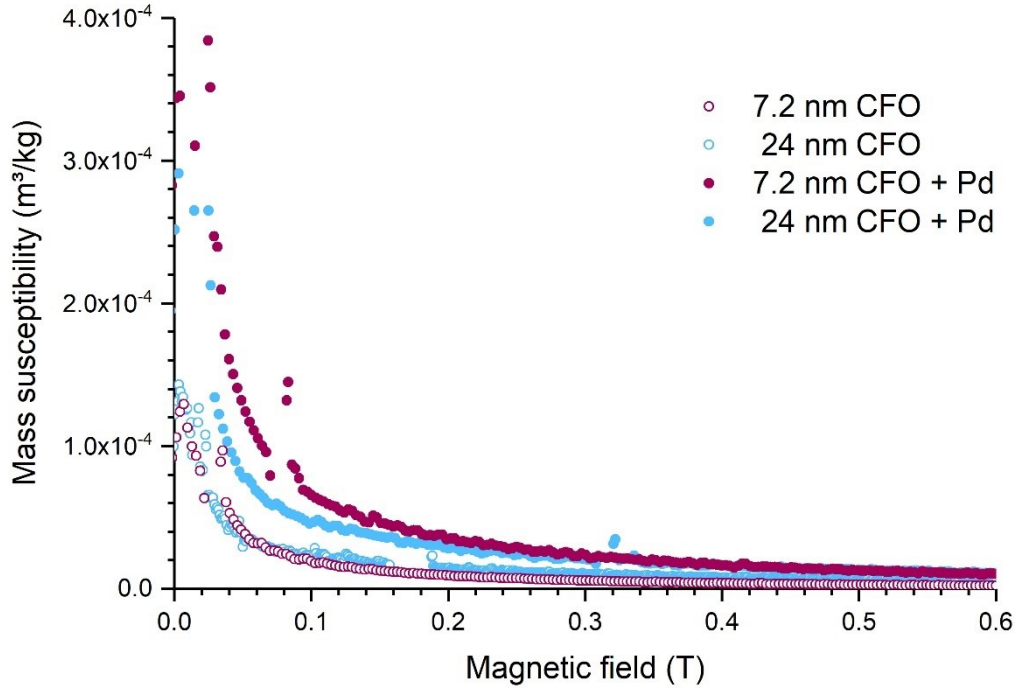


Figure S4. Mass susceptibility at  $T = 300$  K extracted from the magnetometry data shown in Fig. S2.

Table S4. Simulation parameters used for fitting experimental data (Fig. S2) with the law of approach (Eq. S1) and the extracted effective anisotropy.

| Composition | $d_H$ (nm) | $M_s$ ( $\text{Am}^2/\text{kg}$ ) | $\beta$ ( $\text{T}^2$ ) | $\chi_p$ | $K_{\text{eff}}$ ( $\text{J}/\text{kg}$ ) |
|-------------|------------|-----------------------------------|--------------------------|----------|---|
| CFO         | 7.2        | 7.06                              | 0.273                    | 0.206    | 7.1                                       |
| CFO         | 24.1       | 13.6                              | 1.08                     | 0.352    | 27  |
| CFO-Pd      | 7.2        | 30.3                              | 0.768                    | 0.551    | 51  |
| CFO-Pd      | 24.1       | 27.3                              | 1.09                     | 0.620    | 55  |

### S3. Optimization

In this work, based on the central composite design (CCD) approach, the response surface methodology (RSM) was used to optimize the influence of synthesis parameters on defined responses. 20 experimental runs were carried out for ranges of particle size of between 7.20 and 40 nm, as listed in Table S1. The SAR values of the samples were optimized based on two factors: first, parameters describing the synthesis process, such as reaction temperature, pH and the cation ratio of the magnetic elements (Fe and Co) and, second, structural properties, such as degree of

crystallinity, crystallite size and cation distribution. During optimization, the temperature, pH and cation ratio were varied from 75 to 115 °C, 8 to 12 and 0.45 to 0.55, respectively.

#### S4. SAR difference of the CFO nanoparticle suspension upon repeated runs

Differences between SAR values were determined from two consecutive MFH measurements for CFO suspensions with four ranges of particle size (11.04, 12.17, 14.77 and 15.70 nm). Figure S5 shows that the measured difference values are below 3% (< 0.7 W/g), confirming the reliability of the measurements. In this figure, the approximate measurement uncertainty is 2%.

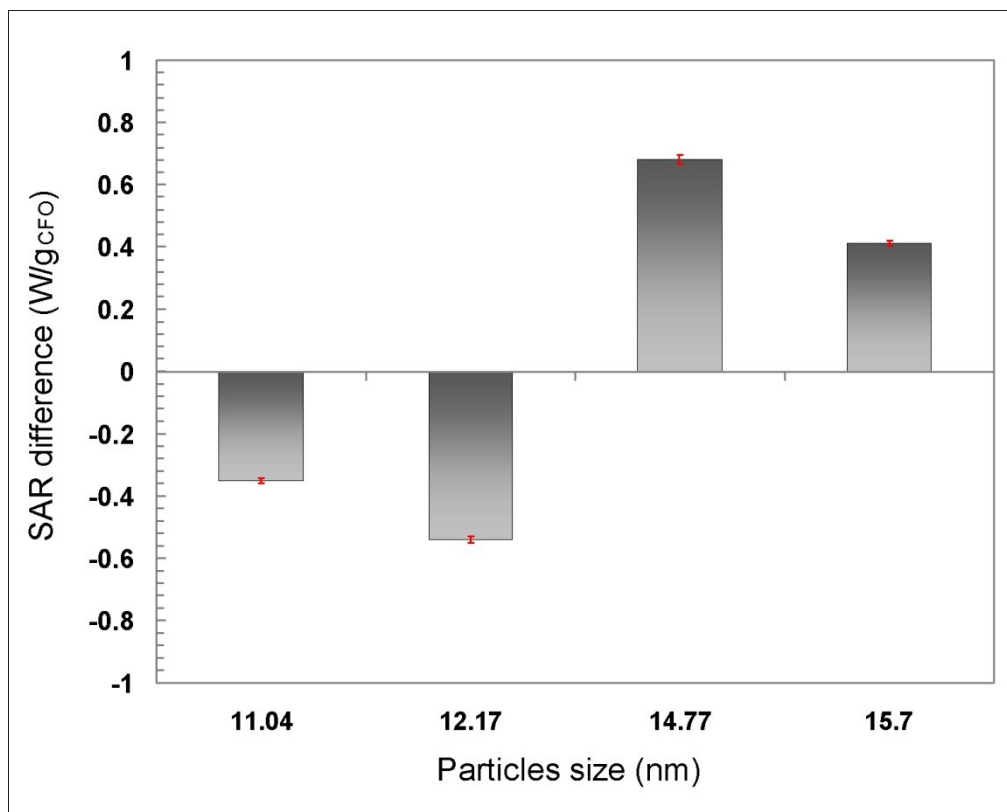


Figure S5. Differences between SAR values obtained from two consecutive MFH measurements for CFO suspensions with different particles sizes. The fluid concentration, magnetic field amplitude and frequency were 15 mg/ml, 19 mT and 318 kHz, respectively.

#### References

- S1. Grössinger, R. Critical Examination of the Law of Approach to Saturation (I). *phys. stat. sol. (a)* 1981, 66, 665.